CHEMISTRY
A EUROPEAN JOURNAL

DOI: 10.1002/chem.200801567

Tuning Glutamine Binding Modes in Gd-DOTA-Based Probes for an Improved MRI Visualization of Tumor Cells

Rachele Stefania,[a] Lorenzo Tei,[b] Alessandro Barge,[c] Simonetta Geninatti Crich,[a] Ibolya Szabo,[a] Claudia Cabella,[d] Giancarlo Cravotto,[c] and Silvio Aime*[a]

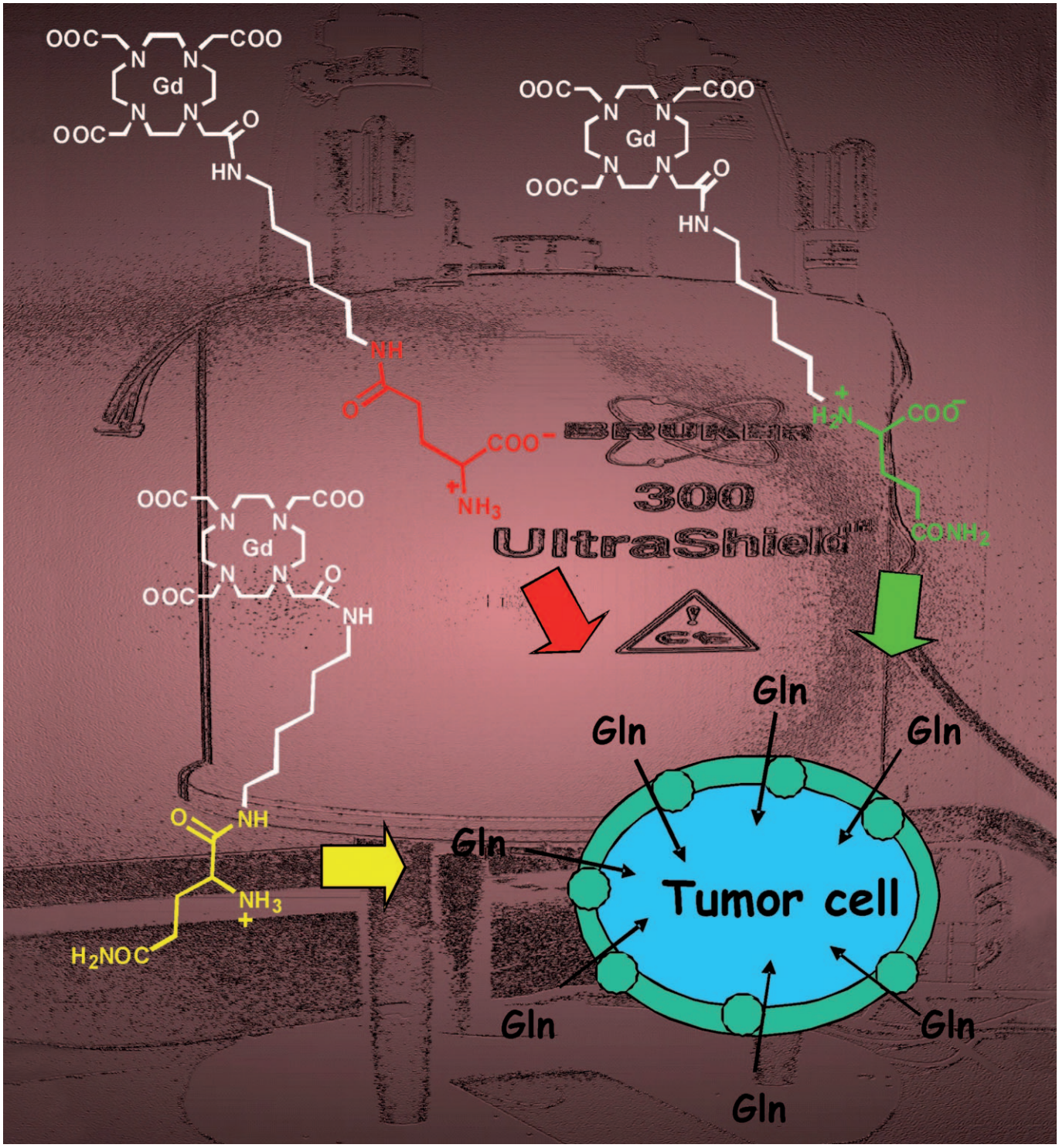

Abstract: Three new magnetic resonance imaging probes that target glutamine transporters have been synthesized. They consist of a Gd-DOTA-monoamide moiety (DOTA = 1,4,7,10-tetraazacyclododecane-1,4,7,10-tetraacetic acid) linked through a six carbon atom chain to a vector represented by a glutamine residue bound through α-carboxylic, γ-carboxamidic, or α-amino functionalities. Their uptake by HTC (rat hepatocarcinoma) and healthy rat hepatocytes has shown that the system containing the glutamine vector bound through the α-carboxylic group displays a markedly higher affinity for tumor cells. The observed behavior is rationalized in terms of the exploitation of an additional glutamine transporter active in hepatic tumor cells.

Keywords: gadolinium · glutamine · hepatoma cells · imaging agents · magnetic resonance imaging

Introduction

Molecular imaging is a rapidly growing field that provides noninvasive visual representation, characterization, and quantification of fundamental biological processes in intact living organisms. Its aims are to widen the detection horizon of early medical diagnoses and to monitor the effects of therapeutic treatments by reporting on the earliest physiological and biochemical events that characterize a given disease.[1–3]

Magnetic resonance (MR) offers the unique opportunity to obtain images characterized by a superb anatomical resolution and to map simultaneously structure and function in soft tissues in vivo. MR is therefore considered a particularly important and advantageous modality for molecular imaging applications. To enhance the sensitivity of MR molecular imaging protocols proper amplification procedures have to be designed in order to deliver a high number of imaging reporting units at the target site.[4] This task of accumulating a large number of contrast agent (CA) molecules at the target site has been pursued, for instance, by means of gadolinium-loaded targeted liposomes,[5–8] targeted iron oxide nanoparticles,[9,10] and perfluorocarbon nanoparticles.[11,12] A potential problem of these large constructs, however, is that their size may prevent them from escaping the blood circuit to reach the sites of interest.

[a] Dr. R. Stefania, Dr. S. Geninatti Crich, Dr. I. Szabo, Prof. S. Aime
Dipartmento di Chimica IFM and Molecular Imaging Center
Università di Torino, Via Nizza 52, 10125 Torino (Italy)
Fax: (+39) 011-670-6487
E-mail: silvio.aime@unito.it

[b] Dr. L. Tei
Dipartimento di Scienze dell'Ambiente e della Vita (DiSAV)
Università del Piemonte Orientale "A. Avogadro"
Via Bellini 25/G, 15100 Alessandria (Italy)

[c] Dr. A. Barge, Prof. G. Cravotto
Dipartimento di Scienza e Tecnologia del Farmaco
Università di Torino, Via P. Giuria 9, 10125 Torino (Italy)

[d] Dr. C. Cabella
Bracco Imaging SpA
via Ribes 5, 10010 Colleretto Giacosa (TO) (Italy)

Supporting information for this article is available on the WWW under http://dx.doi.org/10.1002/chem.200801567. It contains a description of HPLC Methods 1–7 used for the purification and characterization of final products.

Recently, we reported that it is possible to accumulate a sufficient number of small gadolinium-based imaging probes in tumor cells by exploiting their amino acid transporting systems, in particular the glutamine (Gln) transporters.[13,14] The increased expression or up-regulation of the amino acid transporters, particularly Gln transporters, is strictly related to cell growth and it can be considered as a good marker for tumor cells.[15,16] In fact, rapidly growing cells use Gln as a nitrogen, carbon, and energy source. In a previous study, we synthesized a Gd-DOTA-monoamide derivative bearing a Gln residue separated from the chelating moiety by a C_6 aliphatic chain. In vitro and in vivo experiments demonstrated that this probe is taken up by tumor cells. In this imaging probe the Gln vector is linked through an amidic bond between its α-amino group and the carboxylic residue present in the aliphatic chain spacer (Gd-DOTAMAC_6Gln in Scheme 1; DOTAMA = DOTA-monoamide). This binding scheme alters the Gln charge distribution in respect of the free amino acid as it transforms the primary α-amino group into a secondary amide. Moreover, the latter group displays enhanced rigidity and hindrance, which decreases its overall recognition capabilities towards the Gln transporter. A definitive optimization of the design of the Gln-bearing probe may come from the knowledge of the three-dimensional transporter structure, which is, to date, unknown. To overcome this lack of information we decided to synthesize new probes in which Gln is bonded to the contrast enhancing unit through other functional groups (carboxylic, amino, and carboxamide groups) and to test their targeting capabilities towards tumor cells to select the most effective system. Bonding through the α-carboxylic, γ-carboxamidic, or α-amino functionalities led to three new systems, namely, Gd-DOTAMAC_6Glnα (Gd-**L1**), Gd-DOTAMAC_6Glnγ (Gd-**L2**), and Gd-DOTAMAC_6GlnA (Gd-**L3**), in addition to the previously reported Gd-DOTAMAC_6Gln (Scheme 1).

Results and Discussion

Probe design: In the previously reported Gd-DOTA-MAC_6Gln probe,[13] the bonding to the imaging reporter implied the transformation of an amino into an amide functionality, which would compromise the contribution of one of the possible Gln recognition sites on its transporting pro-

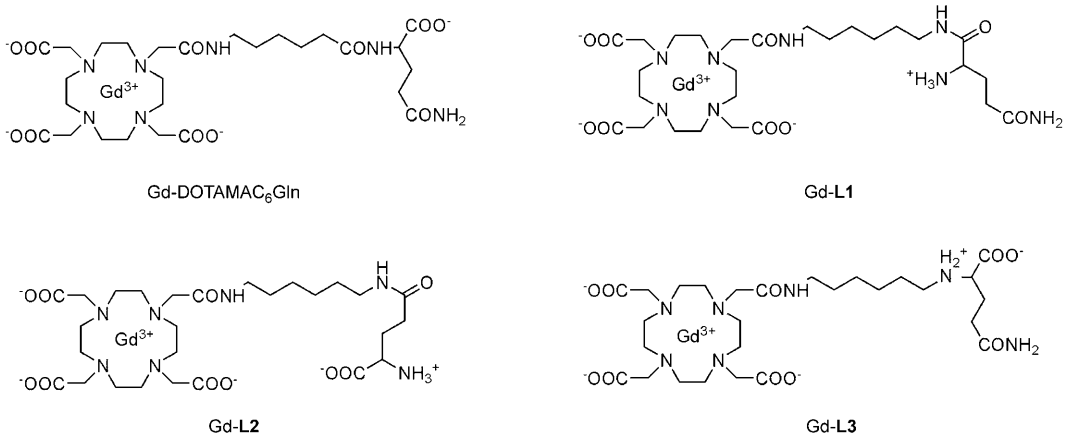

Scheme 1. Structures of the glutamine-containing probes.

teins. In fact, conversely to what occurred for the neutral zwitterionic amino acid Gln, the presence of a free carboxylate group results in an overall negative charge at physiological pH. Because the structural details are not yet known, we have designed three imaging probes in which the Gln moiety is attached to the DOTAMA unit by one of the three other functional groups to gain a better understanding of the recognition target determinants of the membrane transporter. The new probes, Gd-**L1**, Gd-**L2**, and Gd-**L3**, maintain the same DOTA-monoamide chelating unit and the C_6 aliphatic spacer of Gd-DOTAMAC$_6$Gln, but the use of different binding sites endows the Gln residue with quite different structural properties and overall charge at physiological pH.

In Gd-**L1** the Gln is attached to the imaging reporter through its carboxylic group, thereby forming an amidic bond, as in Gd-DOTAMAC$_6$Gln. At physiological pH, the targeting moiety of the probe differs from the parent Gln amino acid because it displays an overall positive charge, the α-amino group being protonated and the carboxylic group being replaced by a secondary amide.

Instead, in Gd-**L2** the anchor point is the primary γ-amide of Gln, which yields a zwitterionic neutral form at physiological pH. However, although the charge distribution of the Gln vector is unaltered, in this probe the amino acid loses its characteristic terminal amide functional group, which in principle could be important in the recognition by the Gln transporter.

Finally, Gd-**L3** was designed in such a way that the Gln moiety would remain unaltered as much as possible. For this reason, the α-amino group of a protected Gln derivative was subjected to reductive amination with the bifunctional chelating agent DOTAMAC$_5$CHO to obtain a secondary amine in place of the primary α-amino group of the parent amino acid. At physiological pH, the Gd-**L3** probe is present as a zwitterion and has the same charge distribution as in Gln, although the isoelectric point is slightly higher as a consequence of the occurrence of the secondary, more basic, amine. Furthermore, the secondary amine is more hindered than in Gln and this hindrance could interfere in the binding to the transporter.

Synthesis: Two bifunctional chelating agents containing a free amino or an aldehydic group separated from the coordinating cage by a hexamethylene aliphatic chain were used for the synthesis of ligands **L1**, **L2**, and **L3**. Namely, DOTAMA(O*t*Bu)$_3$C$_6$NH$_2$ was used for the synthesis of **L1** and **L2** and DOTAMA(O*t*Bu)$_3$C$_5$CHO for the synthesis of **L3** (Schemes 2 and 3). The synthesis of these DOTAMA-functionalized building blocks has been recently reported.[17]

L1 and **L2** were synthesized by the reaction of DOTAMA(O*t*Bu)$_3$C$_6$NH$_2$ with the pentafluorophenyl-activated esters of *N*-Boc-L-glutamine and *N*-Boc-L-glutamic α-*tert*-butyl ester, respectively, followed by acid hydrolysis of the protecting groups (Scheme 2).

L3 was synthesized by reductive amination between DOTAMA(*t*Bu)$_3$C$_5$CHO and a Gln derivative protected as the *tert*-butyl ester on the carboxylic acid and as the *N*-trityl secondary amide (H$_2$N-L-Gln(Tr)-O*t*Bu) (Scheme 3). This protected Gln was synthesized in three steps starting from the benzyloxycarbonyl (Cbz)-protected Gln.

Following a literature procedure,[18] the terminal amide was protected as the trityl amide by reaction with triphenylmethanol, acetic anhydride, and sulfuric acid. Then the carboxylic acid was protected as the *tert*-butyl ester by acid-catalyzed transesterification with *tert*-butyl acetate and the final H$_2$N-L-Gln(Tr)-O*t*Bu was obtained by hydrogenolysis of the Cbz group under pressure (50 bar, 50 °C). The reductive amination between H$_2$N-L-Gln(Tr)-O*t*Bu and DOTAMA(O*t*Bu)$_3$C$_5$CHO was carried out under ultrasound (US) irradiation for 30 min (20 W, 20 kHz) in MeOH at controlled pH (pH 5); sonication was continued for another 30 min after the addition of triacetoxyborohydride. The reaction conditions had to be carefully optimized to avoid the hydrolysis of the amide bond between the spacer and the DOTA unit, which would result in a series of byproducts and a reduction in the yield. The yields were invariantly very low when this reaction was carried out under conven-

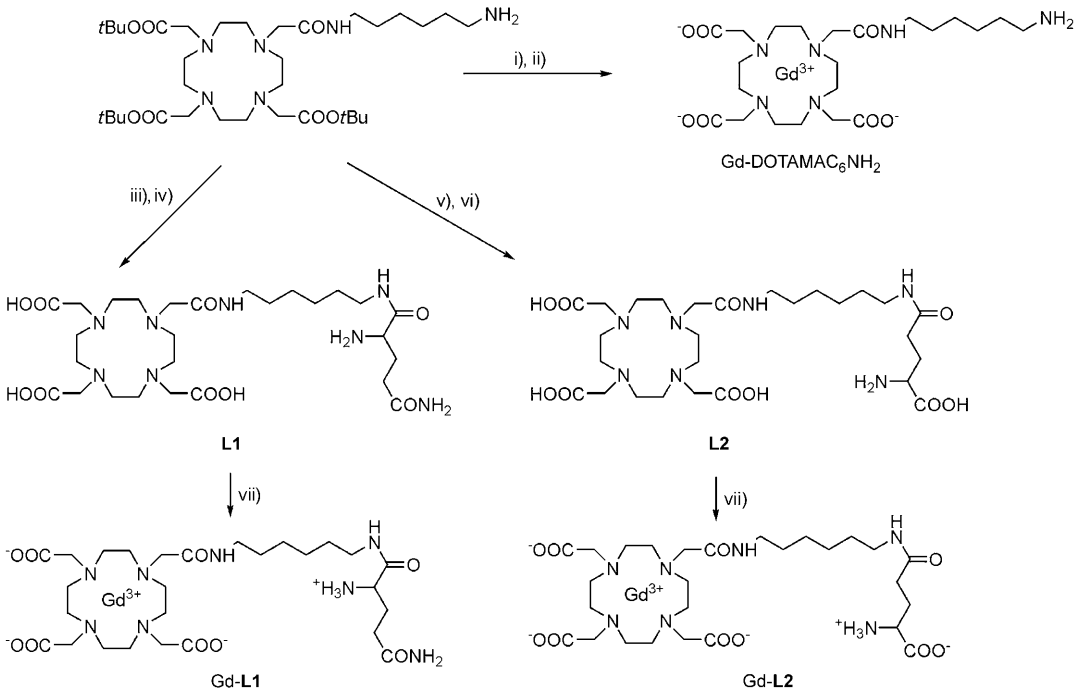

Scheme 2. Synthetic pathways to $GdDOTAMAC_6NH_2$, Gd-$DOTAMAC_6Gln\alpha$ (Gd-**L1**), and Gd-$DOTAMAC_6Gln\gamma$ (Gd-**L2**). i) TFA, CH_2Cl_2; ii) $GdCl_3$, H_2O, pH 7; iii) Boc-L-Gln-OH, DCC/Pfp, CH_2Cl_2 to give **1**; iv) TFA, CH_2Cl_2; v) Boc-L-Glu(O*t*Bu)-OH, DCC/Pfp, CH_2Cl_2 to give **2**; vi) TFA, CH_2Cl_2; vii) $GdCl_3$, H_2O, pH 7.

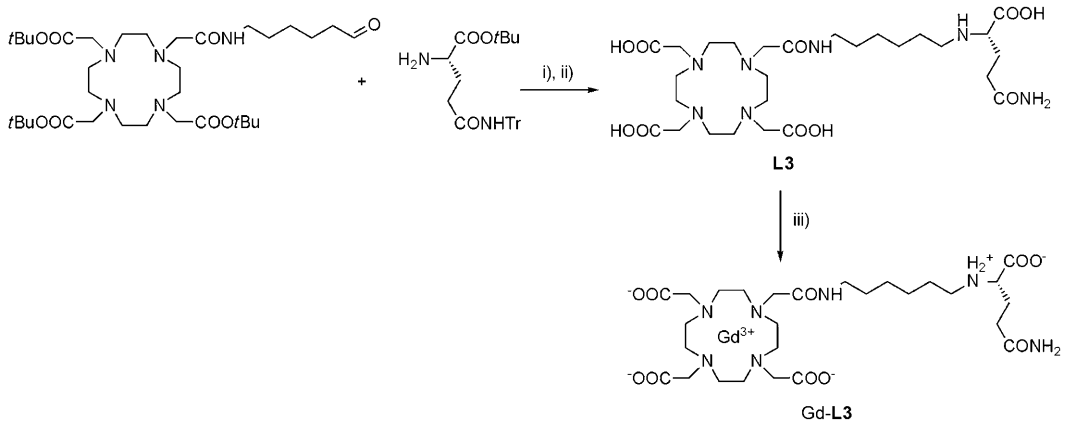

Scheme 3. Synthetic pathway to Gd-$DOTAMAC_6GlnA$ (Gd-**L3**). i) $NaBH(OAc)_3$, AcOH, ultrasound (20 W), CH_3OH to give **3**; ii) TFA, CH_2Cl_2; iii) $GdCl_3$, H_2O, pH 7.

tional conditions. However, sonication allows a dramatic improvement of the yields, as observed in other reported reductive amination procedures.[19,20]

Whereas in the case of **L2**, cleavage of the Boc and *tert*-butyl protecting groups with trifluoroacetic acid gave the product in good yields, in the cases of **L1** and **L3**, TFA catalyzed an intramolecular transamination reaction between the α-amino group and the amide of the Gln with the formation of a 5-oxopyrrolidine ring (**L4** and **L5**) and ammonia (Scheme 4). This clearly causes a dramatic change in the structural characteristics of the vector moiety.

This cyclization is particularly favored by the formation of a five-membered pyrrolidinic ring and is known to occur with Gln under hydrolytic conditions, especially in the presence of bivalent cations and Brønsted or Lewis acids and bases.[21] In fact, glutamic and pyroglutamic acids (5-oxopyrrolidine-2-carboxylate) have been reported to be glutamine metabolites, which shows that the intramolecular reaction can also occur in vivo.[22,23] Moreover, Gln as the *N*-terminal amino acid in many proteins, hormones, and neurotransmitter peptides has been found to cyclize intramolecularly either spontaneously or under the action of enzymes such as glutaminyl cyclase.[24,25] With the intramolecular cyclization process being such an easy process, the *tert*-butyl ester hydrolysis reaction was monitored by ESI-MS every 30 min in order to stop it before too much of the cyclic byproduct was

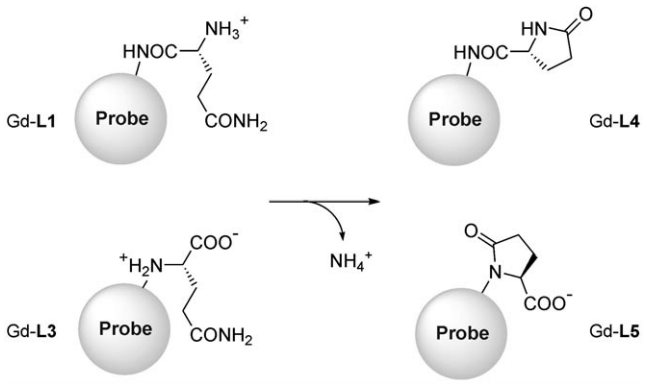

Scheme 4. Glutamine cyclization reaction on probe surfaces.

formed. **L1** and **L4** were recovered after purification by semipreparative HPLC–MS in about 40 and 25% yields, respectively. A similar result was found for **L3** and **L5**. Because **L1** and **L3** are prone to cyclization at both acidic and basic pHs, we had to find the optimal conditions for HPLC separation. A reversed-phase column and a gradient with 7 mM ammonium acetate buffer at pH 4 and acetonitrile as eluents provided the best conditions to minimize the unwanted transformation in the separation medium. The pH had to be kept at slightly acidic values because separation of the linear and cyclic products was not possible at neutral pH. However, immediately after separation, the fractions containing pure **L1** or **L3** had to be neutralized with a solution of NH_4OH to avoid further cyclization. After complexation with $GdCl_3$, a second HPLC purification procedure (water/acetonitrile gradient elution) was carried out to remove salts from the products. Taking into account the tendency of **L1** and **L3** to cyclize in the presence of metal ions, it was found useful to skip the purification step for the ligands and to just purify the final complexes. These purifications were carried out by semipreparative HPLC–MS with a water/acetonitrile gradient elution. Yields of about 40% were obtained for the linear complexes and of about 25% for the cyclic ones.

Synthesis and relaxometric characterization of gadolinium complexes: The Gd^{III} complexes were prepared by mixing stoichiometric amounts of the DOTAMA-containing probes and $GdCl_3$ solution. In the case of Gd-**L2**, unchelated Gd^{3+} ions were eliminated by precipitation of the hydroxide at basic pH by adding aliquots of a concentrated NaOH solution. The amount of free Gd^{III} was determined by UV spectrophotometry.[26] Finally, excess gadolinium was eliminated by adding a stoichiometric amount of the ligand. In the cases of Gd-**L1** and Gd-**L3**, to avoid the cyclization of Gln catalyzed by basic pH and/or trivalent cations, unchelated Gd^{3+} was eliminated by the addition of 0.5 equiv of iminodiacetic acid followed by LC–MS purification using H_2O and CH_3CN as eluents (see the Supporting Information). The relaxivities (the proton relaxation enhancement of water protons in the presence of the paramagnetic complex at a concentration of 1 mM) measured at 20 MHz and 298 K for Gd-**L1**, Gd-**L2**, and Gd-**L3** were 5.6, 5.6, and 5.5 $mM^{-1}s^{-1}$, respectively. These values are in agreement with those previously reported for a number of analogous gadolinium complexes with variously substituted DOTA-monoamide ligands.[27] These values are slightly higher than that reported for the parent Gd-DOTA complex ($r_{1p}=4.7\ mM^{-1}s^{-1}$) as a consequence of the increased molecular weight.[28]

Cell uptake experiments: The affinity of the different Gln-containing gadolinium complexes for the rat hepatoma cell line (HTC) was determined and compared with that observed for the previously reported Gd-DOTAMAC_6Gln complex.[13] The procedure used in this study consisted of incubating around 1.5 million cells for 6 h at 37 °C in a minimum medium (Earl's balanced salt solution: EBSS) containing the gadolinium complexes at a concentration of 1 mM. After incubation the cells were washed three times with ice-cold phosphate-buffered saline (PBS) and detached from the culture flasks mechanically with a cell scraper. Figure 1

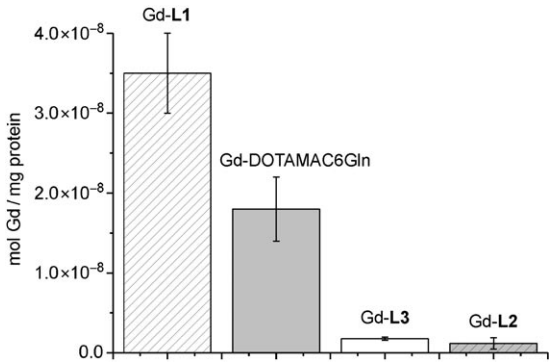

Figure 1. Internalization of gadolinium complexes functionalized with Gln by HTC cells. For the uptake experiment, about 1.5 million cells were incubated at 37 °C for 6 h in EBSS with Gd-**L1**, Gd-**L2**, Gd-**L3**, and Gd-DOTAMaC_6Gln at concentrations of 1 mM.

shows that the compound bearing a free amino group (Gd-**L1**) displays an improved uptake by tumor cells, of about 200%, compared with that previously reported for Gd-DOTAMAC_6Gln. In contrast, the bonding of Gln through the primary γ-amide group in Gd-**L2** led to a dramatic decrease in affinity for tumor cells. Also the uptake of Gd-**L3**, although present as a zwitterion and with the same functional groups and charge distribution as Gln, was significantly lower.

T_1-weighted spin echo MR images of cells (Figure 2) showed that only after the incubation of Gd-**L1** and Gd-DOTAMAC_6Gln were the amounts of internalized gadolinium sufficient to generate hyperintensity in the corresponding MR images.

To assess whether the high affinity of Gd-**L1** for tumor cells relies on the presence of a positive charge, the nonspecific precursor Gd-DOTAMAC_6NH_2 was incubated with HTC cells under the same conditions (6 h, 37 °C, EBSS). The number of moles of gadolinium per mg of protein taken

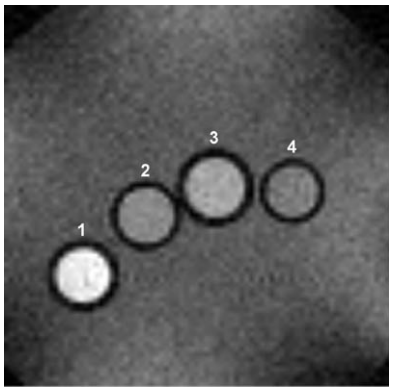

Figure 2. T_1-weighted spin-echo MR image (measured at 7 T) of an agar phantom containing HTC cells incubated for 6 h at 37 °C with 1) Gd-**L1,** 2) Gd-**L3,** 3) Gd-DOTAMA-C_6-Gln, and 4) Gd-**L2**.

up was 50 times lower (about 7×10^{-10}) than that measured after incubation with Gd-**L1**, which indicates that the presence of Gln on the complex surface is essential for its specific interaction to tumor cells. Further evidence that Gln was the vehicle for the internalization through the amino acid transporting system was obtained by incubating HTC cells for 3 h in the presence of 0.25 mM Gd-**L1** with or without an excess of Gln. In the presence of 10 mM Gln the number of moles of gadolinium taken up per mg of protein was 75% lower than that measured in its absence, which demonstrates the specific internalization pathway.

The unexpected behavior of the two probes that have the same charge distribution and functional groups in Gln (Gd-**L2** and Gd-**L3**) could be ascribed to the significant modification introduced into the vector structure by the binding to the MRI reporter. We suggest that such a modification of the Gln structure compromises its interaction with appropriate transporters. However, the presence of a positive or negative localized charge on the other two probes (Gd-**L1** and Gd-DOTAMAC_6Gln) may reduce this unfavorable effect, probably because of the formation of electrostatic interactions between the vector and transporter.

Hepatoma cells transport Gln at a rate 10–20 times faster than normal hepatocytes[29] as a consequence of the expression of an additional transport system that does not occur in normal hepatocytes. In fact, in human hepatoma cell lines, Gln is transported through the cytoplasmatic membrane by both the system commonly expressed on hepatocytes (system N) and by a different system that has only subsequently been elucidated.[30] This system differs from ASC (the transport system that mediates Gln transport in many tumor cell lines) due to its interaction with basic amino acids. This observation may account for the increased internalization of the basic Gd-**L1** complex compared with other probes investigated in this work. In fact, the presence of the free amino group appears to facilitate the interaction with the negatively charged domains of the protein transporter on the cell membrane.

The uptake of the more efficient Gd-**L1** was determined with the primary culture of rat hepatocytes and compared with that observed with hepatoma cells. To this end, rat hepatocytes and HTC cells were incubated for 6 h in the presence of 1 mM Gd-**L1**. Figure 3A shows that HTC cells labeled with Gd-**L1** display a hyperintense signal in the T_1-weighted spin-echo image compared with the unlabeled cells. In contrast, the signal intensity of the healthy rat hepatocytes is only slightly greater than the signal intensity of the unlabeled cells. In fact, in this case, the amount of gadolinium internalized (1 nmol of gadolinium per mg of protein) is about 35 times lower than that found for hepatoma cells (Figure 3B). As a consequence of the increased uptake of Gd-**L1** by tumor cells, there is around a 350% enhancement in the intensity of the hepatocytes of the rat hepatoma when compared with the pellet of cells derived from healthy rat liver.

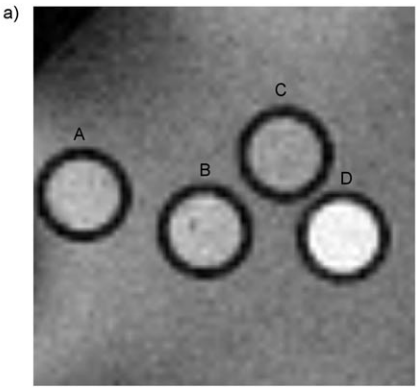

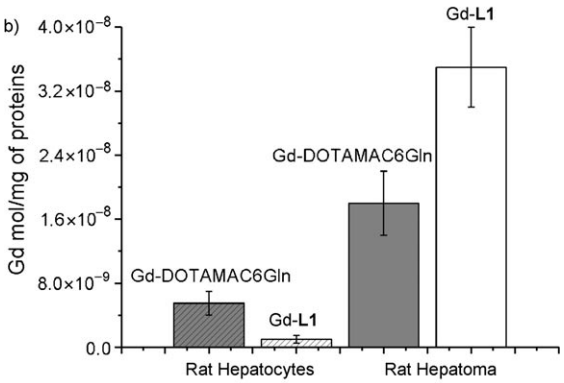

Figure 3. a) T_1-weighted spin-echo MR image (measured at 7 T) of an agar phantom containing A) unlabeled hepatocytes, B) hepatocytes labeled with Gd-**L1**, C) unlabelled HTC, and D) HTC labeled with Gd-**L1**. b) Comparison of the internalization of Gd-L1 and Gd-DOTAC_6Gln into rat hepatocytes and hepatoma (HTC). Cells were incubated for 6 h in the presence of 1 mM gadolinium complex solutions in EBSS.

Comparison of Gd-**L1** with the previously reported negatively charged Gd-DOTAMAC_6Gln showed a significant increase in the tumor/healthy cell ratio of internalized gadolinium. In fact, the amount of Gd-**L1** taken up by hepatoma cells is about 35 times higher than the amount of Gd-**L1** taken up by healthy hepatocytes, whereas the amount of Gd-DOTAMAC_6Gln taken up was about 10 times lower.

This is a direct consequence of the contrasting behavior observed with the positively charged amino acid of transport systems expressed on tumor and normal cells (system N), respectively.

Afterwards, the internalization by hepatoma cells of Gd-**L1** was compared with that observed with its cyclic derivative (Scheme 4) as a function of complex concentration in the incubation media. Figure 4 shows that intramolecular Gln cyclization reduces significantly the amount of gadolinium internalized in the range of concentrations investigated as a consequence of the change in the vector structure.

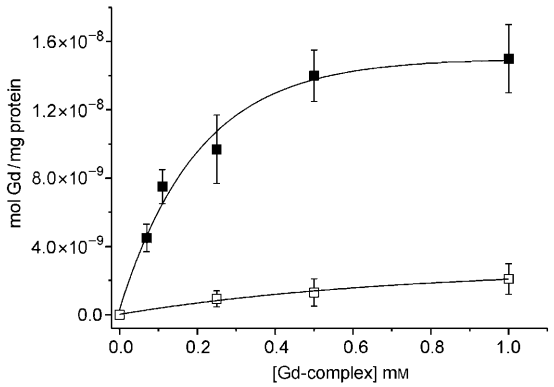

Figure 4. Internalization by HTC cells of Gd-**L1** (■) and its cyclic derivative Gd-**L4** (□). Cells were incubated for 6 h at 37 °C with increasing concentrations (0.07–1 mM) of the two gadolinium complexes.

This observation is particularly important in the development of systems that exploit Gln as a carrier for tumor cells because undetected cyclization can reduce markedly the probe uptake in target cells. For this reason it is useful to obtain an estimate of the ratio of the cyclic and linear form of Gd-**L1** by an appropriate analytical HPLC method (see Method 7 in the Supplementary Information). Furthermore, the asymptotic shape of the curve observed for Gd-**L1** indicates the occurrence of an active internalization mechanism.

Conclusion

Modulation of the binding scheme through which a Gln residue is bound to the surface of a MR imaging reporter has allowed a system that is avidly taken up by hepatoma tumor cells to be identified. The differences observed in the internalization of this probe into HTC and healthy hepatocytes illustrates the important role of a transporter devoted to the uptake of basic amino acids that is peculiar to hepatic tumors. The amount of gadolinium-based probe Gd-**L1** that is taken up by HTC cells is twice as large as that previously reported for Gd-DOTAC$_6$Gln and markedly higher than that for the other Gln-based probes developed in this work. The results obtained represent a step forward in the development of MR molecular imaging applications based on the accumulation of a high number of gadolinium chelates at the target cells due to the exploitation of high capacity transporters. The new insights gained in this work add further support to the overall armory of tools available for MR visualization of tumor cells.[31–33]

Experimental Section

All chemicals were purchased from Sigma-Aldrich Co. and were used without purification unless otherwise stated. NMR spectra were recorded on JEOL Eclipse Plus 400 and Bruker Avance 600 spectrometers (operating at 9.4 and 14 T, respectively). The sonochemical apparatus used in this work was developed by the authors in collaboration with Danacamerini s.a.s. (Torino).[19,34] ESI mass spectra were recorded on a Waters Micromass ZQ spectrometer. Analytical and preparative HPLC–MS were carried out on a Waters FractionLynx autopurification system equipped with Waters 2996 diode array and Micromass ZQ (ESCI ionization mode) detectors. DOTAMA(O*t*Bu)$_3$C$_6$NH$_2$ and DOTAMA-(O*t*Bu)$_3$C$_5$CHO were prepared following a reported procedure.[17] The longitudinal water proton relaxation rate was measured on a Stelar Spinmaster spectrometer (Stelar, Mede, Italy) operating at 20 MHz using the standard inversion–recovery technique (16 experiments, 2 scans). A typical 90° pulse width was 3.5 μs and the reproducibility of the T_1 data was ±0.5%.

Tri-*tert*-butyl ester of (*S*)-1-[2,11-dioxo-12-(*tert*-butoxycarbonylamino)-14-carbamoyl-3,10-diazatetradecanyl]-1,4,7,10-tetraazacyclododecane-4,7,10-triacetic acid (1): A solution of dicyclohexylcarbodiimide (DCC) (1.3 g, 6.56 mmol) in CH_2Cl_2 (20 mL) was added to a stirred solution of *N*-Boc-L-Gln-OH (1.47 g, 5.96 mmol) in CH_2Cl_2 (80 mL) that had been cooled to 0 °C. Pentafluorophenol (Pfp) (1.2 g, 6.56 mmol) was added and the mixture was stirred at 0 °C for 3 h and then for another 16 h at room temperature. The solvent was partly removed and precipitated dicyclohexylurea (DCU) was filtered off. The filtrate was added dropwise to a solution of DOTAMA(O*t*Bu)$_3$C$_6$NH$_2$ (4 g, 5.96 mmol) in CH_2Cl_2 (50 mL). The mixture was allowed to react overnight at room temperature, the solvent was removed under reduced pressure, and the residue purified by column chromatography (silica gel, elution gradient: CH_2Cl_2/MeOH, 95:5→9:1→8:2→7:3; TLC: CH_2Cl_2/MeOH, 9:1 (v/v), R_f=0.22) to yield a slightly yellow oil (2.4 g, 44.8%). ^{1}H NMR (400 MHz, $CDCl_3$): δ=8.63 (br, CONH, 1H), 7.93 (br, CONH, 1H), 7.56, (br, CONH, 1H), 4.29 (m, CH_α, 1H), 3.50–3.20, 3.10–2.07 (br, CH_2 macrocycle, NCH_2CO, $CONHCH_2$, $CH_{2\beta}$, $CH_{2\gamma}$, 36H), 1.53–1.28 ppm (br, $C(CH_3)_3$, aliphatic CH_2, 40H); ^{13}C NMR (400 MHz, $CDCl_3$): δ=176.1, 172.4, 172.2, 172.1, 171.4, 155.8 (CONH, COO, 6C), 81.8, 79.1 ($C(CH_3)_3$, 4C), 56.1, 55.7, 55.6, 54.5, 53.5 (NCH_2CO, NCH_2 macrocycle, 12C), 50.0 (CH_α,1C), 38.8, 38.7 ($CONHCH_2$, 2C), 32.4, 29.6, 29.0, 28.9 (aliphatic CH_2, $CH_{2\beta}$, CH_γ, 4C), 28.4, 27.9 ($C(CH_3)_3$, 12C), 26.0, 25.9 ppm (aliphatic CH_2, 2C); MS (ESI+): *m*/*z*: calcd for $C_{44}H_{83}N_8O_{11}$ $[M+H]^+$: 899.62; found: 899.91.

(*S*)-1-(2,11-Dioxo-12-amino-14-carbamoyl-3,10-diazatetradecanyl)-1,4,7,10-tetraazacyclododecane-4,7,10-triacetic acid (L1): Compound **1** (1.00 g, 1.11 mmol) was dissolved in CH_2Cl_2 (10 mL), trifluoroacetic acid (35 mL) and triisopropylsilane (0.6 mL) were added, and the mixture was stirred at room temperature for 2 h. The reaction was monitored by ESI-MS every 30 min to avoid any delay that would favor cyclization. The mixture was then evaporated in vacuo and the product precipitated with excess diethyl ether. The product was isolated by centrifugation, washed thoroughly with diethyl ether, and dried in vacuo. It was then dissolved in H_2O (5 mL) and the pH neutralized by addition of dilute NH_4OH at 0 °C. The crude product was purified by preparative HPLC–MS by using a Waters Atlantis RPdC18 19/100 column by Method 1 using 7 mM CH_3COONH_4 (pH 4) (A) and CH_3CN (B) as eluents (see the Supporting Information). A second fast chromatographic separation was needed to eliminate salts (Method 2, see the Supporting Information). The pure product was obtained as a white powder (270 mg, 39%). ^{1}H NMR (600 MHz, D_2O): δ=3.92 (m, CH_α,1H), 3.76–3.70 (br, CH_2 macrocycle, 4H), 3.49, 3.32 (br, CH_2 macrocycle, 12H), 3.18–2.97 (br, NCH_2CO, $CONHCH_2$, CH_2NH, 12H), 2.36 (m, $CH_{2\beta}$, 2H), 2.08 (m, $CH_{2\gamma}$, 2H),

1.46, 1.26 ppm (m, aliphatic CH_2, 8H); ^{13}C NMR (600 MHz, D_2O): $\delta =$ 176.4, 175.6, 170.3, 169.2, 167.8 (CONH and COO, 5C), 55.6, 54.6, 54.3, 51.6 (NCH_2CO, CH_α, 5C), 50.6, 49.9, 47.2 (NCH_2 macrocycle, 8C), 38.4, 38.1 ($CONHCH_2$, 2C), 29.1, 27.1, 25.5, 24.7, 22.8, 22.4 ppm (aliphatic CH_2, $CH_{2\beta}$, CH_{γ}, 6C); MS (ESI+): *m/z*: calcd for $C_{27}H_{51}N_8O_9$ $[M+H]^+$ 631.38; found: 631.62.

(*S*)-1-[6-(5-Oxopyrrolidin-2-ylcarbonylamino)hexylcarbamoylmethyl]-1,4,7,10-tetraazacyclododecane-4,7,10-triacetic acid (L4)—cyclic product: The cyclized product (153 mg, 25% yield) was recovered by HPLC separation. ^1H NMR (600 MHz, D_2O): $\delta = 4.23$ (m, CH_α, 1H), 3.81–3.68 (br, CH_2 macrocycle, 4H), 3.43, 3.38 (br, CH_2 macrocycle, 12H), 3.18–3.01 (br, NCH_2CO, $CONHCH_2$, CH_2NH, 12H), 2.97 (m, $CH_{2\beta}$, 2H), 2.37 (m, $CH_{2\gamma}$, 2H), 1.46, 1.26 ppm (m, aliphatic CH_2, 8H); MS (ESI+): *m/z*: calcd for $C_{27}H_{48}N_7O_9$ $[M+H]^+$: 614.35; found: 614.58.

Tetra-*tert*-butyl ester of (*S*)-1-[2,11-dioxo-14-(*tert*-butoxycarbonylamino)-14-carboxy-3,10-diazatetradecanyl]-1,4,7,10-tetraazacyclododecane-4,7,10-triacetic acid (2): A solution of DCC (1.4 g, 7.26 mmol) in CH_2Cl_2 (80 mL) was added to a stirred solution of Boc-L-Glu(O*t*Bu)-OH (2.0 g, 6.6 mmol) in CH_2Cl_2 (80 mL) under cooling at 0°C. Then pentafluorophenol (1.3 g, 7.26 mmol) was added and the mixture stirred at 0°C for 3 h and for another 16 h at room temperature. After filtration of the precipitated DCU, the solvent was partly removed and the solution was filtered again to remove some more DCU. The filtrate was added dropwise to a solution of $DOTAMA(OtBu)_3C_6NH_2$ (4.4 g, 6.6 mmol) in CH_2Cl_2 (50 mL). After the mixture had been allowed to react overnight at room temperature, the solvent was removed under reduced pressure and the residue was purified by column chromatography (silica gel, elution gradient: CH_2Cl_2/MeOH, 95:5→9:1→8:2→7:3; TLC: CH_2Cl_2/MeOH, 9:1 (v/v), $R_f = 0.20$) to yield a slightly yellow oil (3.2 g, 53.9%). ^1H NMR (400 MHz, $CDCl_3$): $\delta = 8.73$ (br, CONH, 1H), 8.35 (br, CONH, 1H), 7.82, (br, CONH, 1H), 4.05 (m, CH_α,1H), 3.45–3.10, 2.95–1.80 (br, CH_2 macrocycle, NCH_2CO, $CONHCH_2$, $CH_{2\beta}$, $CH_{2\gamma}$, aliphatic CH_2, 36H), 1.51–1.28 ppm (br, $C(CH_3)_3$, aliphatic CH_2, 49H); ^{13}C NMR (400 MHz, $CDCl_3$): $\delta = 174.0$, 173.9, 172.6, 172.5, 172.1, 172.0, 156.9 (CONH, COO, 7C), 81.5, 82.4, 80.7 ($C(CH_3)_3$, 5C), 58.2, 58.1, 56.1, 56.2, (NCH_2CO, CH_α, 5C), 55.5, 55.0, 54.0, 53.5 (NCH_2 macrocycle, 8C), 40.4, 40.3 ($CONHCH_2$, 2C), 34.2, 30.6, 30.4, (aliphatic CH_2, $CH_{2\beta}$, $CH_{2\gamma}$, 4C), 30.1, 28.9, 28.8 ($C(CH_3)_3$, 15C), 28.0, 27.9 ppm (aliphatic CH_2, 2C); MS (ESI+): *m/z*: calcd for $C_{48}H_{89}N_7NaO_{12}$ $[M+Na]^+$: 978.65; found: 979.11.

(*S*)-1-(2,11-Dioxo-14-amino-14-carboxy-3,10-diazatetradecanyl)-1,4,7,10-tetraazacyclododecane-4,7,10-triacetic acid (L2): Compound **2** (1.50 g, 1.66 mmol) was dissolved in CH_2Cl_2 (15 mL), trifluoroacetic acid (15 mL) and triisopropylsilane (0.6 mL) were added, and the mixture was stirred at room temperature overnight. The liquid was then evaporated in vacuo and the product precipitated with excess diethyl ether. The product was isolated by centrifugation, washed thoroughly with diethyl ether, and dried in vacuo to yield the desired product as an amorphous white solid. This was purified by preparative HPLC–MS by using a Waters Atlantis RPdC18 19/100 column by Method 3 and H_2O/0.1% TFA (A) and CH_3CN/0.1% TFA (B) as eluents (see the Supporting Information). The pure product was obtained as a white powder (0.9 g, 89.9%). ^1H NMR (600 MHz, D_2O): $\delta = 3.68$ (m, CH_α, 1H), 3.40–2.57 (br, CH_2 macrocycle, NCH_2CO, $CONHCH_2$, CH_2NH, 16H), 2.91–2.55 (br, CH_2 macrocycle, 12H), 2.10 (m, $CH_{2\beta}$, 2H), 1.85(m, $CH_{2\gamma}$, 2H), 1.15, 0.95 ppm (m, aliphatic CH_2, 8H); ^{13}C NMR (600 MHz, D_2O): $\delta = 173.7$, 171.6, 170.3, 169.5, 164.8 (CONH, COO, 6C), 65.97, 54.7 (NCH_2CO, CH_α, 5C), 52.5, 52.0, 51.3, 47.5 (NCH_2 macrocycle, 8C), 39.2, 39.0 ($CONHCH_2$, 2C), 30.9, 27.9, 27.8, 26.9, 25.7, 25.4, 25.3 ppm (aliphatic CH_2, $CH_{2\beta}$, $CH_{2\gamma}$, 6C); MS (ESI+): *m/z*: calcd for $C_{27}H_{50}N_7O_{10}$ $[M+H]^+$: 632.36; found: 632.57.

***N*-Cbz-L-Gln(Tr)-OH**: Cbz-L-Gln-OH (1 g, 3.57 mmol) and Tr-OH (1.86 g, 7.14 mmol) were suspended in glacial acetic acid (11 mL). Ac_2O (0.7 mL, 7.14 mmol) and H_2SO_4 (0.02 mL, 0.36 mmol) were added and the reaction mixture was stirred for 1 h under N_2 at 50°C (bath temperature) to form a clear yellow solution. The reaction mixture was dropped into cold water (110 mL) and the precipitate was filtered, dissolved in EtOAc (30 mL), and washed with H_2O (3×10 mL). The organic phase was dried with Na_2SO_4 and the solvent was evaporated under reduced pressure. The product was dissolved in EtOAc (50 mL) and dropped into hexane (200 mL). The precipitated product was separated by centrifugation to obtain a white powder (0.94 g, 50%). ^1H NMR (400 MHz, $CDCl_3$): 7.26 (m, 20H), 5.09 (s, 2H), 4.16 (m, 1H), 2.51 (m, 1H), 2.38 (m, 1H), 2.02 ppm (m, 2H); MS (ESI+): *m/z*: calcd for $C_{32}H_{31}N_2O_5$ $[M+H]^+$: 523.22; found: 523.31.

***N*-Cbz-L-Gln(Tr)-O*t*Bu**: *N*-Cbz-L-Gln(Tr)-OH (5 g, 9.55 mmol) was suspended in *t*BuOAc (64 mL, 0.478 mol) in a round-bottomed flask. $HClO_4$ (0.164 mL, 1.91 mol) was slowly added dropwise into the reaction mixture, which was stirred for 20 h at RT. A light-yellow suspension resulted and the reaction was monitored by TLC (silica, CH_2Cl_2/MeOH, 9:1, $R_{f,product} = 0.95$). Aqueous Na_2CO_3 (10%, 40 mL) was slowly added to the reaction mixture. The solution was transferred to a separating funnel and EtOAc (100 mL) was added. The water phase was separated, its pH was adjusted to 10 by adding aqueous NaOH (1M, ca. 22 mL), and then it was returned to the organic phase in the separating funnel and thoroughly shaken. The organic phase was washed with H_2O (3×100 mL), dried with Na_2SO_4, and the solvent was removed under reduced pressure. The product was purified by column chromatography (stationary phase: silica; mobile phase: gradient starting from CH_2Cl_2 (100 mL), then CH_2Cl_2/MeOH 95:5). Yield: 74%. ^1H NMR(400 MHz, $CDCl_3$): $\delta = 7.26$ (m, 20H), 5.09 (s, 2H), 4.22 (m, 1H), 2.41 (m, 1H), 2.33 (m, 1H), 2.16 (m, 1H), 1.86 (m, 1H), 1.42 ppm (s, 9H); MS (ESI+): *m/z*: calcd for $C_{36}H_{39}N_2O_5$ $[M+H]^+$: 579.28; found: 579.3.

H_2N-L-Gln(Tr)-O*t*Bu: *N*-Cbz-L-Gln(Tr)-O*t*Bu (2 g, 3.47 mmol) was placed in a PARR reactor, dissolved in dioxane (60 mL), and water-moistened 10% Pd/C (0.3 g) was added. The mixture was stirred under hydrogen pressure (50 bar) at 50°C for about 24 h. The reaction was checked by TLC (silica, CH_2Cl_2/MeOH, 9:1, $R_{f,product} = 0.32$, $R_{f,reactant} = 0.95$). The resulting solution was first filtered, then run through a short column of silica gel. This was washed with methanol to recover all the product retained on the silica gel. The solvent was removed under reduced pressure. Yield: 84%. ^1H NMR (400 MHz, $CDCl_3$): $\delta = 7.26$ (m, 15H), 3.30 (m, 1H), 2.41 (m, 2H), 2.08 (m, 1H), 1.75 (m, 1H), 1.41 ppm (s, 9H); MS (ESI+): *m/z*: calcd for $C_{28}H_{33}N_2O_3$ $[M+H]^+$: 445.25; found: 445.32.

Tri-*tert*-butyl ester of (*S*)-1-[2-oxo-11-(*tert*-butoxycarbonyl)-13-(*N*-tritylcarbamoyl)-3,10-diazaterdecanyl]-1,4,7,10-tetraazacyclododecane-4,7,10-triacetic acid (3): A solution of $DOTAMA(OtBu)_3C_5CHO$ (1.8 g, 2.73 mmol) in CH_3OH (10 mL) was adjusted to pH 5 with glacial acetic, then NH_2-L-Gln(Tr)-O*t*Bu (1.2 g, 2.73 mmol) dissolved in CH_3OH (10 mL) was added. The mixture was transferred to a glass cylinder and sonicated in a cup horn at 20 W for 20 min. $NaBH(OAc)_3$ was then added portionwise and the mixture sonicated for another 30 min. The resulting solution was evaporated in vacuo and the residue dissolved in H_2O/$CHCl_3$ (30 mL, 1:1 (v/v)). Dilute aqueous NH_4OH was added under stirring at 0°C to adjust the pH to 8, then the organic phase was separated and the aqueous phase extracted with $CHCl_3$ (3×30 mL). The organic phases were collected, dried with anhydrous Na_2SO_4, filtered, and evaporated in vacuo. The residue was purified by column chromatography (silica gel, eluent: $CHCl_3$/MeOH, 9:1; TLC: $R_f = 0.36$) to yield a light-yellow oil (1.4 g, 49%). ^1H NMR (400 MHz, $CDCl_3$): $\delta = 8.51$ (br, CONH, 1H), 8.08 (br, CONH, 1H), 7.26–7.18 (m, ArH, 15H), 3.46 (m, CH_α, 1H), 3.41–3.26 (br, CH_2 macrocycle, NCH_2CO, $CONHCH_2$, CH_2NH, 28H), 2.34 (m, $CH_{2\beta}$, 2H), 2.29 (m, $CH_{2\gamma}$, 2H), 1.41 (m, $C(CH_3)_3$, 36H), 1.46, 1.43, 1.24 ppm (m, aliphatic CH_2, 8H); ^{13}C NMR (400 MHz, $CDCl_3$): $\delta = 172.7$, 172.3, 171.8, 171.7, 171.6 (CONH, COO, 6C), 145.04, 128.8, 127.9, 126.6 (aromatic, 15C), 82.0, 81.9, 81.8 ($C(CH_3)_3$, 4C), 70.6 ($C(Ph)_3$, 1C), 61.5 (CH_α, 1C), 56.4, 56.0, 55.9, 53.9 (NCH_2CO, NCH_2 macrocycle, 12C), 48.0 ($NHCH_2$, 1C), 39.5 ($CONHCH_2$, 1C), 34.3, 32.8, 29.7 (aliphatic CH_2, $CH_{2\beta}$, 3C), 28.7, 28.4, 28.3, 28.2 ($C(CH_3)_3$, 12C), 27.6, 27.2, 26.3 ppm (aliphatic CH_2, $CH_{2\gamma}$, 3C); MS (ESI+): *m/z*: calcd for $C_{62}H_{96}N_7O_{10}$ $[M+H]^+$: 1098.72; found: 1099.03; calcd for $C_{62}H_{95}N_7NaO_{10}$ $[M+Na]^+$: 1120.70; found: 1121.02.

(*S*)-1-(2-Oxo-11-carboxy-13-carbamoyl-3,10-diazaterdecanyl]-1,4,7,10-tetraazacyclododecane-4,7,10-triacetic acid (L3): Trifluoroacetic acid (20 mL) was added dropwise to a solution of **3** (337 mg, 0.30 mmol) and triisopropylsilane (0.6 mL) in CH_2Cl_2 (5 mL) cooled to 0–5°C. The solution was stirred at room temperature for 1 h, then evaporated, and the residue dissolved in the same volumes of CH_2Cl_2 and trifluoroacetic acid.

After 2 h, the solvent volume was reduced and the product precipitated by adding diethyl ether at 0–5 °C. The precipitate was dissolved in H_2O (5 mL), the solution neutralized at 0–5 °C by adding dilute aqueous NH_4OH, and finally lyophilized. The product was then purified by preparative HPLC–MS by using a Waters Atlantis RPdC18 19/100 column by Method 4 and 7 mM CH_3COONH_4 (pH 4) (A) and CH_3CN (B) as eluents (see the Supporting Information). A second fast chromatographic separation was needed to eliminate salts (Method 2, Supporting Information). The pure product was obtained as a white powder (270 mg, 39 %). ^{1}H NMR (600 MHz, D_2O): $\delta = 3.82–3.69$ (br, CH_2 macrocycle, 4H), 3.57 (m, CH_α, 1H), 3.42–3.34 (br, CH_2 macrocycle, 12H), 3.14–2.96 (br, NCH_2CO, $CONHCH_2$, CH_2NH, 12H), 2.38 (m, $CH_{2\beta}$, 2H), 2.15–2.02 (m, $CH_{2\gamma}$, 2H), 1.66, 1.47, 1.32 ppm (m, aliphatic CH_2, 8H); ^{13}C NMR (600 MHz, D_2O): $\delta = 178.8$, 176.9, 175.9, 175.8, 170.9 (CONH, COO, 6C), 60.2 (CH_α, 1C), 59.9, 55.0 (NCH_2CO, 4C), 53.5, 51.1, 48.1, 46.6 (NCH_2 macrocycle, 8C), 41.8 (CH_2NH, 1C), 39.2 ($CONHCH_2$, 1C), 30.4, 29.6, 28.0, 27.8, 25.8, 25.7 ppm (aliphatic CH_2, $CH_{2\beta}$, $CH_{2\gamma}$, 6C); MS (ESI+): *m/z*: calcd for $C_{27}H_{50}N_7O_{10}$ $[M+H]^+$: 632.36; found: 632.51; calcd for $C_{27}H_{49}N_7NaO_{10}$ $[M+Na]^+$: 654.34; found: 654.5.

(*S*)-1-[6-(2-Carboxy-5-oxopyrrolidin-1-yl)hexylcarbamoylmethyl]-1,4,7,10-tetraazacyclododecane-4,7,10-triacetic acid (L5)—cyclic product: The cyclized product (123 mg, 20 %) was recovered by HPLC separation. ^{1}H NMR (600 MHz, D_2O): $\delta = 4.40$ (m, CH_α, 1H), 3.92–3.64 (br, CH_2 macrocycle, 4H), 3.42–3.10 (br, CH_2 macrocycle, NCH_2CO, $CONHCH_2$, CH_2NH, 24H), 2.45–2.34 (m, $CH_{2\beta}$, 2H), 2.12–2.02 (m, CH_γ, 2H), 1.46, 1.26 ppm (m, aliphatic CH_2, 8H); MS (ESI+): *m/z*: calcd for $C_{27}H_{47}N_6O_{10}$ $[M+H]^+$: 615.33; found: 615.41.

Gd^{III} complexes (Gd-L1, Gd-L2, Gd-L3, Gd-L4, Gd-L5, and Gd-DOTA-MAC$_6$NH$_2$: An equimolar amount of $GdCl_3$ solution (about 120 mM in water) was slowly added to a 40 mM ligand solution; the solutions were maintained at pH 7 with NaOH.

In the cases of Gd-**L1** and Gd-**L3**, iminodiacetic acid (0.5 equiv) was added after 2 h to complex free Gd^{3+} ions. The mixtures were stirred overnight at RT and lyophilized to give a white solid. Then Gd-**L1** and Gd-**L3** were purified by preparative HPLC–MS by Methods 5 and 6, respectively, using a Waters Atlantis RPdC18 19/100 column and H_2O (A) and CH_3CN (B) as eluents (see the Supporting Information). Starting from crude **L1** and **L3** (i.e., also containing **L4** and **L5**, respectively), the same protocol was used, but this time Gd-**L4** and Gd-**L5** were also obtained after HPLC purification.

In the cases of Gd-**L2** and Gd-**DOTAMAC$_6$NH$_2$**, the mixtures were stirred overnight at RT. Then the pH was raised to 8.5 and the mixtures stirred for 2 h. Centrifugation at 7000 rpm for 5 min at 10 °C allowed the separation of $Gd(OH)_3$ from solution.

The amount of residual free Gd^{3+} ions was assessed by the Orange Xylenol UV method.[26] All complexes used in this work were found to contain less than 0.3 % (mol/mol) of residual free Gd^{3+} ions. The overall gadolinium contents were determined by ^{1}H NMR T_1 measurement of the mineralized complex solution (in 6 M HCl at 120 °C for 16 h).

Gd-L1: MS (ESI+): *m/z*: calcd for $C_{27}H_{48}GdN_8O_9$ $[M+H]^+$: 786.28; found: 786.74; HPLC: Method 7 (see the Supporting Information), retention time 2.83 min, purity 96 %.

Gd-L4: MS (ESI+): *m/z*: calcd for $C_{27}H_{45}GdN_7O_9$ $[M+H]^+$: 769.25; found: 769.65; HPLC: Method 7, retention time 4.70 min, purity 80 %.

Gd-L2: MS (ESI+): *m/z*: calcd for $C_{27}H_{47}GdN_7O_{10}$ $[M+H]^+$: 787.26; found: 787.68; HPLC: Method 7, retention time 3.16 min, purity 95 %.

Gd-L3: MS (ESI+): m/z: calcd for $C_{27}H_{47}GdN_7O_{10}$ $[M+H]^+$: 787.26; found: 787.51; HPLC: Method 7, retention time 2.08 min, purity 84 %.

Gd-L5: MS (ESI+): *m/z*: calcd for $C_{27}H_{44}GdN_6O_{10}$ $[M+H]^+$: 770.24; found: 770.61; HPLC: Method 7, retention time 3.27 min, purity 80 %.

For all complexes the signals observed show isotopic distribution consistent with a gadolinium complex. The products were stored at −20 °C to prevent cyclization.

Cell culture: The culture media DMEM F-12, M199, and fetal bovine serum (FBS) were purchased from Cambrex, East Rutherford, NJ, USA. The penicillin–streptomycin mixture, serum bovine albumin (BSA), trypsin, glutamine, and all other chemicals were purchased from Sigma Chemical Co., St. Louis, MO, USA. Rat hepatocytes were isolated by following the previously reported method[35,36] and were used for the uptake experiments after 24 h of culture. HTC (rat hepatoma tissue culture) were grown in DMEM F-12 medium supplemented with 5 % FBS, 2 mM glutamine, 100 U mL^{-1} penicillin, and 100 μg mL^{-1} streptomycin. HTC were cultured in 75 cm^2 flasks in a humidified incubator in CO_2/air (5:95, v/v) at 37 °C. For the uptake experiments HTC cells were seeded at a density of 1.5×10^4 cells cm^{-2}. Cells were ready for the uptake experiments 24 h after seeding.

Uptake experiments: To carry out the uptake experiments with the gadolinium complexes, HTC and rat hepatocytes were seeded in 6 and 10 cm diameter culture dishes, respectively. After removal of the culture medium, cells were washed three times with phosphate saline buffer (PBS) (5 mL) and then Earl's Balanced Salt Solution (2 or 5 mL; EBSS: $CaCl_2$ 0.266 g L^{-1}, KCl 0.4 g L^{-1}, NaCl 6.8 g L^{-1}, glucose 1 g L^{-1}, $MgSO_4$ 0.204 g L^{-1}, NaH_2PO_4 0.144 g L^{-1}, $NaHCO_3$ 1.1 g L^{-1}, pH 7.4) were added to the 6 or 10 cm dishes, respectively. Cells were incubated (5 % CO_2 at 37 °C) for 6 h with the different compounds dissolved in EBSS at a 1 mM concentration. At the end of the incubation, the medium was removed and cells were washed three times with ice-cold PBS. Then cells were recovered from the Petri dishes in 250 μL PBS with a cell scraper. The gadolinium content of the HTC was determined by using inductively coupled plasma mass spectrometry (ICP-MS, Element-2, Thermo-Finnigan, Rodano (MI), Italy). Sample digestion was performed with concentrated HNO_3 (70 %, 2 mL) under microwawe heating (Milestone MicroSYNTH Microwave labstation equipped with an optical fiber temperature control and a HPR-1000/6M six-position high-pressure reactor, Bergamo, Italy). After digestion the volume of each sample was brought to 2 mL with ultrapure water, and the samples were analyzed by ICP-MS. Three replicates of each sample solution were analyzed. The protein concentration of each sample was determined from cell lysates by the Bradford method using bovine serum albumin as the standard.

MRI: MR images of cell pellets were acquired on a Bruker Avance 300 (7 T) instrument equipped with a microimaging probe. The system was endowed with two birdcage resonators of 30 and 10 mm inner diameter, respectively. 1.5×10^6 HTC cells were incubated for 6 h with equal amounts (1 mM) of the different gadolinium complexes. 5×10^6 rat hepatocytes were incubated for 6 h with Gd-**L1**. At the end of the incubation, cells were washed three times with ice-cold PBS, detached with EDTA (1 mM), and transferred into glass capillaries for the analysis. MR imaging was performed by using a standard T_1-weighted multislice multiecho sequence (TR/TE/NEX = 200:3.3:16, field of view = 1.2 cm, one slice = 1 mm, in-plane resolution = 94×94 μm). T_1 measurements of cells were performed by using a standard saturation recovery sequence.

Acknowledgements

This work was supported by the EC-FP6 (MEDITRANS: NMP4-CT-2006-026668; DiMI: LSHB-CT-2005-512146, and EMIL: LSHC-CT-2004-503569) and by the Italian Government (project nos. FIRB RBNE03PX83_006, FIRB RBIP06293N, and PRIN 2005039914). EC-COST D38 Action is also acknowledged.

[1] T. F. Massoud, S. S. Gambhir, *Trends Mol. Med.* **2007**, *13*, 183–191.
[2] R. Weissleder, M. J. Pittet, *Nature* **2008**, *452*, 580–589.
[3] K. Brindle, *Nat. Rev. Cancer* **2008**, *8*, 94–107.
[4] S. Aime, S. Geninatti Crich, E. Gianolio, G. B. Giovenzana, L. Tei, E. Terreno, *Coord. Chem. Rev.* **2006**, *250*, 1562–1579.
[5] W. J. Mulder, G. J. Strijkers, G. A. van Tilborg, A. W. Griffioen, K. Nicolay, *NMR Biomed.* **2006**, *19*, 142–164.
[6] N. Kamaly, T. Kalber, A. Ahmad, M. H. Oliver, P. W. So, A. H. Herlihy, J. D. Bell, M. R. Jorgensen, A. D. Miller, *Bioconjugate Chem.* **2008**, *19*, 118–129.

[7] S. Erdogan, Z. O. Medarova, A. Roby, A. Moore, V. P. Torchilin, *J. Magn. Reson. Imaging* **2008**, *27*, 574–580.
[8] K. F. Pirollo, J. Dagata, P. Wang, M. Freedman, A. Vladar, S. Fricke, L. Ileva, Q. Zhou, E. H Chang, *Mol. Imaging* **2006**, *5*, 41–52.
[9] S. Laurent, D. Forge, M. Port, A. Roch, C. Robic, L. Vander Elst, R. N. Muller, *Chem. Rev.* **2008**, *108*, 2064–2110.
[10] C. Corot, P. Robert, J. M. Idee, M. Port, *Adv. Drug Delivery Rev.* **2006**, *58*, 1471–1504.
[11] S. D. Caruthers, P. M. Winter, S. A. Wickline, G. M. Lanza, *Methods Mol. Med.* **2006**, *124*, 387–400.
[12] T. D. Tran, S. D. Caruthers, M. Hughes, J. N. Marsh, T. Cyrus, P. M. Winter, A. M. Neubauer, S. A. Wickline, G. M. Lanza, *Int. J. Nanomed.* **2007**, *2*, 515–526.
[13] S. Geninatti Crich, C. Cabella, A. Barge, S. Belfiore, C. Ghirelli, L. Lattuada, S. Lanzardo, A. Mortillaro, L. Tei, M. Visigalli, G. Forni, S. Aime, *J. Med. Chem.* **2006**, *49*, 4926–4936.
[14] L. Lattuada, S. Demattio, V. Vincenzi, C. Cabella, M. Visigalli, S. Aime, S. Geninatti Crich, E. Gianolio, *Bioorg. Med. Chem. Lett.* **2006**, *16*, 4111–4114.
[15] W. W. Souba, *Ann. Surg.* **1993**, *218*, 715–728.
[16] M. A. Medina, *J. Nutr.* **2001**, *131*, 2539S-2542S.
[17] A. Barge, L. Tei, D. Upadhyaya, F. Fedeli, L. Beltrami, R. Stefanìa, S. Aime, G. Cravotto, *Org. Biomol. Chem.* **2008**, *6*, 1176–1184.
[18] P. Sieber, B. Rineker, *Tetrahedron Lett.* **1991**, *32*, 739–742.
[19] G. Cravotto, G. Omiccioli, L. Stevanato, *Ultrason. Sonochem.* **2005**, *12*, 213–217.
[20] A. Barge, G. Cravotto, B. Robaldo, E. Gianolio, S. Aime, *J. Inclusion Phenom. Macrocyclic Chem.* **2007**, *57*, 489–495.
[21] V. R. Young, A. M. Ajami, *J. Nutr.* **2001**, *131*, 2449S–2459S.
[22] B. D. Ross, S. Bullock, *Biochem. J.* **1978**, *170*, 177–179.
[23] G. Chen, J. B. Russell, *J. Bacteriol.* **1989**, *171*, 2981–2985.
[24] R. W. Garden, T. P. Moroz, J. M. Gleeson, P. D. Floyd, L. Li, S. S. Rubakhin, J. V. Sweedler, *J. Neurochem.* **1999**, *72*, 676–681.
[25] W. H. Busby, G. E. Quackenbush, J. Humm, W. W. Youngblood, J. S. Kizer, *J. Biol. Chem.* **1987**, *262*, 8532–8536.
[26] A. Barge, G. Cravotto, E. Gianolio, F. Fedeli, *Contrast Media Mol. Imaging* **2006**, *1*, 184–188.
[27] D. Thonon, V. Jacques, J. F. Desreux, *Contrast Media Mol. Imaging* **2007**, *2*, 24–34.
[28] P. Caravan, J. J. Ellison, T. J. McCurry, *Chem. Rev.* **1999**, *99*, 2293–2352.
[29] B. P. Bode, D. L. Kaminski, W. W Souba, A. P. Li, *Hepatology* **1995**, *21*, 511–520.
[30] J. D. McGivan, *Biochem. J.* **1998**, *330*, 255–260.
[31] C. Li, M. F. Penet, P. Winnard, Jr., D. Artemov, Z. M. Bhujwalla, *Clin. Cancer Res.* **2008**, *14*, 515–522.
[32] P. M. Winter, K. Cai, S. D. Caruthers, S. A. Wickline, G. M. Lanza, *Expert Rev. Med. Devices* **2007**, *4*, 137–145.
[33] A. S. Krishnan, A. A. Neves, M. M. de Backer, D. E. Hu, B. Davletov, M. I. Kettunen, K. M. Brindle, *Radiology* **2008**, *246*, 854–862.
[34] G. Cravotto, A. Dimetri, G. M. Nano, G. Palmisano, A. Penoni, S. Tagliapietra, *Eur. J. Org. Chem.* **2003**, 4438–4444.
[35] G. Gardini, C. Cabella, C. Cravanzola, C. Vargiu, S. Belliardo, G. Testore, S. P. Solinas, A. Toninello, M. A. Grillo, S. Colombatto, *J. Hepatol.* **2001**, *35*, 482–489.
[36] I. Probst, *Eur. J. Biochem.* **1985**, *153*, 347–353.

Received: July 31, 2008
Published online: December 4, 2008

